ISSN 0021-8944, Journal of Applied Mechanics and Technical Physics, 2021, Vol. 62, No. 3, pp. 419–428. © *Pleiades Publishing, Ltd., 2021.*
Russian Text © *S.M. Aulchenko, E.V. Kartaev.*

CONTROL OF GAS-PHASE HIGH-TEMPERATURE SYNTHESIS OF TITANIUM DIOXIDE NANOPARTICLES IN A PLASMA-CHEMICAL REACTOR WITH THE USE OF A QUENCHING JET

S. M. Aulchenko* **and E. V. Kartaev**

UDC 532.075.8

Abstract: The influence of a quenching air jet on physical and chemical properties and morphology of titanium dioxide, silicon dioxide, and TiO_2–SiO_2 composite particles synthesized by the one-stage chloride method in a flow-type plasma-chemical reactor is studied. The results of the simulations and analysis of the samples show that the physical and chemical properties of the powder and the morphology of its particles can be controlled. It is demonstrated that the results of mathematical simulations of the synthesis of TiO_2 and SiO_2 particles agree well with the experimental data obtained in the study.

Keywords: titanium dioxide, silicon dioxide, composite particle, plasma-chemical reactor, one-velocity multispecies medium, homogeneous and heterogeneous reactions, coagulation.

DOI: 10.1134/S0021894421030081

INTRODUCTION

Problems of flow control in fluid dynamics play an important role in various technological developments. One of the first problems of passive control of the gas flow was solved in [1]; modeling of this problem at the Institute of Theoretical and Applied Mechanics of the Siberian Branch of the Russian Academy of Sciences (ITAM SB RAS) was supported by Academician Yanenko. Investigations of the gas-dynamic method of affecting the parameters of the reacting gas mixture and, hence, on the characteristics of the final product, offer much promise for the development of advanced technologies of plasma-chemical synthesis of new materials, including nanostructured powders. In [2–4], where the results of experimental and theoretical studies of conversion of titanium and silicon tetrachloride vapors and synthesis of titanium and silicon dioxide nanoparticles were reported, it was concluded that the size and phase composition of nanoparticles predicted by numerical simulations are in reasonable agreement with the size and phase composition obtained in experiments performed in a laboratory setup for plasma-chemical synthesis of submicron particles by the chloride method. One-stage synthesis of TiO_2–SiO_2 composite nanoparticles by the chloride method with both individual oxidation of titanium and silicon tetrachlorides, i.e., with injection of the mixture of silicon tetrachloride vapor and air far downstream from the region of injection of the mixture of titanium tetrachloride vapor and air, and with joint injection of the reagents was modeled in [5, 6]. The one-stage gas-phase method

Khristianovich Institute of Theoretical and Applied Mechanics, Siberian Branch, Russian Academy of Sciences, Novosibirsk, 630090 Russia; *aulchsm@mail.ru, kartayev@mai.ru. Translated from Prikladnaya Mekhanika i Tekhnicheskaya Fizika, Vol. 62, No. 3, pp. 80–90, May–June, 2021. Original article submitted February 15, 2021; revision submitted March 9, 2021; accepted for publication March 29, 2021.

*Corresponding author.

used in those investigations has some advantages over other methods [7–15]. In particular, gas-phase processes are usually cleaner than liquid-phase processes (because solvents usually contain traces of minerals), and the rate of synthesizing the powder product is appreciably higher, which can ensure batch production. Moreover, it is usually easier to monitor the gas-phase synthesis process and the quality of the final product than in other methods. In the present study, we consider the influence of the quenching air jet on the size of TiO_2 and SiO_2 nanoparticles and also on the size of cores and shells of TiO_2–SiO_2 composite nanoparticles.

The position of the slot for injection of the quenching jet was chosen in such a way that the temperature in the region of mixing of the quenching jet with the main flow did not allow oxygen contained in the jet to act as a reagent. The difference in the flow rates of the reagents in different experiments (and computations) was caused by technical features of injection of $TiCl_4$ and $SiCl_4$ precursor vapors into the reactor, but the sizes of TiO_2, SiO_2, and TiO_2–SiO_2 particles were not compared with each other. The flow rate of the quenching jet was varied only in the case of synthesis of SiO_2 nanoparticles. As a whole, the parameters of the quenching jet were not varied because the goal was not to obtain particles of a specified size.

FORMULATION OF THE PROBLEM

The reactor for synthesis of titanium dioxide, silicon dioxide, and composite nanoparticles is schematically shown in Fig. 1. An air or nitrogen jet with a temperature T_1 and flow rate Q_1 enters the working region through a channel. The first side slot is used to inject a mixture of air with titanium tetrachloride, silicon tetrachloride, or both reagents with a temperature T_2 and flow rate Q_2. In both cases, there is a reaction in the mixing region, which leads to the formation of the TiO_2 (SiO_2) gas-phase component, and then TiO_2 (SiO_2) particles. As the particles move along the reactor channel, their size increases owing to the surface reaction and coagulation. The quenching air jet with a temperature T_3 and flow rate Q_3 can be injected (or not injected) through the second side slot.

In synthesis of composite particles, a nitrogen jet with a temperature T_1 and flow rate Q_1 enters the working region. A mixture of titanium tetrachloride, silicon tetrachloride, and air with a temperature T_2 and flow rate Q_2 is injected through the side slot; the fraction of silicon tetrachloride is several times smaller than the fraction of titanium tetrachloride. Several reactions proceed in the mixing region and further downstream: homogeneous reaction with the formation of the gaseous TiO_2 component, nucleation leading to the formation of monomers of TiO_2 particles, increase in size of these particles owing to the surface reaction and coagulation, and homogeneous reaction with the formation of the gas-phase SiO_2 component, which condenses on the surface of titanium dioxide particles and already formed composite TiO_2–SiO_2 particles. Two models are used in the calculations: model with a completely coated core and model where the fraction of the surface area of each particle in a given volume coated by silicon dioxide is determined [6]. It is assumed that composite particles completely coated by the SiO_2 layer do not coagulate. However, the model implies a possibility of coagulation of particles with a partially coated surface. Both models of synthesis of composite nanoparticles with the structure consisting of a TiO_2 core and SiO_2 shell are based on the experimentally confirmed fact that the time of agglomeration of TiO_2 nanoparticles is smaller by two orders of magnitude than the time of agglomeration of SiO_2 nanoparticles [13].

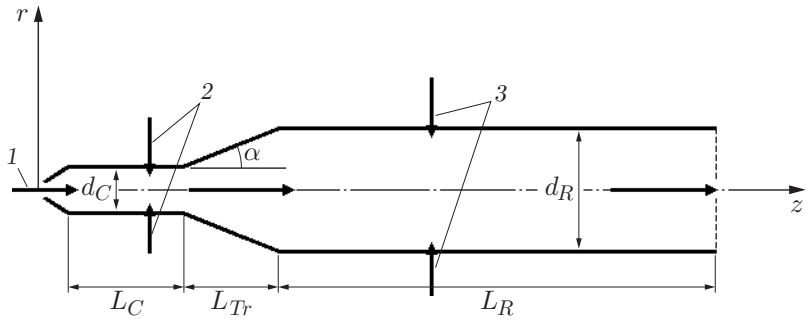

Fig. 1. Working region of the flow reactor with a side jet: (*1*) central jet; (*2*) first side jet; (*3*) second side jet (quenching jet).

In synthesis of composite nanoparticles, the sizes of their cores and shells can be affected by two methods: by varying the ratio of the flow rates of the reagents and by changing the flow regime. The first method does not require structural changes in the setup scheme, but the composition of the final product has to be monitored for each variant. Control of the flow regime (change in temperature, velocity, and density of the flow, generation of additional circulation regions, etc.) is usually ensured with the use of side jets. In this case, their control parameters are the jet injection point and flow rate; in the problem considered here, the control parameter is the composition because the presence or absence of silicon tetrachloride in the side jet corresponds to individual or combined oxidation of the precursors. The flow control variant with individual oxidation of the precursors was considered in [5]. In the present study, in contrast to [5], we consider the influence only of the air jets on the core size and shell thickness.

MATHEMATICAL MODELS

The flow of a viscous heat-conducting mixture of gases is considered. In the case of $TiCl_4$ conversion, the mixture consists of the following species: O_2, N_2, $TiCl_4$, TiO_2, and Cl_2. The last two species are generated in the global chemical reaction

$$TiCl_4 + O_2 \xrightarrow{k_T} TiO_2 + 2Cl_2. \tag{1}$$

In the case of $SiCl_4$ conversion, the mixture consists of O_2, N_2, $SiCl_4$, SiO_2, and Cl_2. The last two species are generated in the global chemical reaction

$$SiCl_4 + O_2 \xrightarrow{k_S} SiO_2 + 2Cl_2. \tag{2}$$

In the case of synthesis of composite particles, the mixture consists of O_2, N_2, $TiCl_4$, $SiCl_4$, TiO_2, SiO_2, and Cl_2. The last three species are generated in the global chemical reactions (1) and (2).

We consider a single-fluid flow described by a system of quasi-gas-dynamic equations [16]. With allowance for external forces and heat sources, this system has the form

$$\frac{\partial \rho}{\partial t} + \operatorname{div} \boldsymbol{j} = 0,$$

$$\frac{\partial (\rho \boldsymbol{u})}{\partial t} + \operatorname{div} (\boldsymbol{j} \otimes \boldsymbol{u}) + \nabla p = \rho \boldsymbol{F} + \operatorname{div} \Pi, \tag{3}$$

$$\frac{\partial E}{\partial t} + \operatorname{div} (\boldsymbol{j} H) + \operatorname{div} \boldsymbol{q} = (\boldsymbol{j} \cdot \boldsymbol{F}) + \operatorname{div} (\Pi \boldsymbol{u}) + Q.$$

Here $\boldsymbol{F}$ is the mass force density vector, H is the total specific enthalpy, and Π is the viscous stress tensor. The mass flux density vector is determined by the expression

$$\boldsymbol{j} = \rho \boldsymbol{u} - \tau [\operatorname{div} (\rho \boldsymbol{u} \otimes \boldsymbol{u}) + \nabla p - \rho \boldsymbol{F}],$$

where $\tau = (M/(\operatorname{Re} \operatorname{Sc}))T/p$, Re is the Reynolds number, and Sc is the Schmidt number. This system is supplemented with the continuity equations for the species of the mixture

$$\frac{\partial \rho_i}{\partial t} + \operatorname{div} \boldsymbol{j}^i = \sum_j J^{(ji)} \tag{4}$$

and the equation for the volume concentration of the solid phase c_p:

$$\frac{\partial c_p}{\partial t} + \operatorname{div} (c_p \boldsymbol{u}) = \sum_j J^{(jp)}. \tag{5}$$

Here $J^{(ji)}$ is the intensity of conversion of the jth species to the ith species, and $J^{(jp)}$ is the intensity of conversion of the jth species to the solid phase. The right sides of Eqs. (4) and (5) in the general case take into account the following kinetic relations, which describe the changes in the concentrations of titanium tetrachloride and titanium dioxide in the gas and solid phases, and also concentrations of silicon tetrachloride and silicon dioxide in the gas and solid phases due to homogeneous and heterogeneous reactions and phase transition:

$$\frac{dC^1}{dt} = -k_T^r C^1 = -(k_T^g + k_T^s A)C^1, \qquad \frac{dC^2}{dt} = k_T^g C^1 - k_T^p C^2,$$

$$\frac{dC^3}{dt} = k_T^s C^1 A + k_T^p C^2, \qquad \frac{dC^4}{dt} = -k_S^r C^4 = -(k_S^g + k_S^s A)C^4, \tag{6}$$

$$\frac{dC^5}{dt} = k_S^g C^4 - k_S^p C^5, \qquad \frac{dC^6}{dt} = k_S^s C^4 A_S + k_S^p C^5.$$

Here C^1, C^2, C^3, C^4, C^5, and C^6 are the concentrations of titanium tetrachloride and titanium dioxide in the gas phase, concentration of titanium dioxide in the solid phase, concentrations of silicon tetrachloride and silicon dioxide in the gas phase, and concentration of silicon dioxide in the solid phase, k_T^r and k_S^r are the rates of the global reactions, k_T^g and k_S^g are the rates of the homogeneous reactions, k_T^s and k_S^s are the rates of the surface reactions, k_T^p and k_S^p are the rates of the phase transitions, and A is the normalized area of the particles.

The additional relations closing the system of equations have the form

$$p = \rho R_m T \frac{m_g}{1 - c_p}, \qquad \alpha_i = \frac{\rho_i}{\rho}, \qquad R_m = R_g \frac{1}{m_i} \sum_i \alpha_i,$$

where R_g is the specific gas constant, R_m is the specific gas constant for the mixture, m_g is the mass fraction of the gas, and α_i is the mass fraction of the ith species.

Supplementing Eqs. (3)–(6) with the equation for the number of particles

$$\frac{dN}{dt} = k_T^g C^1 N_{\mathrm{A}} - \frac{\beta N^2}{2} \tag{7}$$

(N_{A} is the Avogadro number and β is the coagulation parameter [14]) and taking into account the initial diameter d_0, mass, number, and volume concentration of particles at each time instant in each computational cell, one can calculate the particle size.

Following to [14, 15], the values of the constants in Eqs. (6) and (7) were set to

$$k_T^r = 8.26 \cdot 10^4 \, \mathrm{e}^{-10\,681/T}, \qquad k_T^s = 4.9 \cdot 10^3 \, \mathrm{e}^{-8993/T}, \qquad k_T^p = 1.2 \cdot 10^{10} \, \mathrm{e}^{-10\,681/T},$$

$$k_S^r = 8.0 \cdot 10^{14} \, \mathrm{e}^{-400\,000/T}, \qquad k_S^s = 4.0 \cdot 10^{13} \, \mathrm{e}^{-40\,828/T}, \qquad k_S^p = k_T^p.$$

BOUNDARY CONDITIONS

The reactor walls were subjected to the no-slip condition, absence of the heat flux, and zero value of the normal derivative of pressure (this additional condition is caused by the specific feature of the system of quasi-hydrodynamic equations). The conditions for the jets are their flow rates and temperatures. The pressure, density, and velocity at the input boundaries of the jets are calculated by using the boundary conditions based on the Riemann invariants for the Euler equations.

For numerical integration, Eqs. (3)–(5) are written in a cylindrical coordinate system (the problem is axisymmetric) and are converted to the dimensionless form. The governing dimensional parameters of the problem are chosen to be the channel radius, velocity of sound in air at a temperature of 300 K, and air density.

The problem is solved numerically with the use of an explicit difference scheme in time. The derivatives with respect to time are approximated by upwind differences with the first order of accuracy. The derivatives with respect to space are approximated by central differences with the second order of accuracy.

CALCULATION RESULTS

The reactors for synthesis of TiO_2 and SiO_2 nanoparticles have the following geometric parameters: length and diameter $L_R = 444$ mm and $d_R = 32$ mm, respectively, channel length and diameter $L_C = 38$ mm and $d_C = 14$ mm, length of the transitional region $L_{Tr} = 33$ mm, and slope of the side wall of the transitional region $\alpha = 15^\circ$. The coordinates of the middle lines of the slots for side jet injection are $z_1 = 28$ mm and $z_2 = 280$ mm.

The process of titanium tetrachloride conversion was calculated for the following parameters of reactor operation: $T_1 = 3400$ K, $Q_1 = 1$ g/s, $T_2 = 490$ K, $Q_2 = 1.87$ g/s, $T_3 = 300$ K, and $Q_3 = 3.6$ g/s. Figure 2 shows the distributions of the temperature averaged over the cross section and the mean weighted particle diameter (based on the number of particles) along the reactor channel in the presence of the quenching jet and after its interruption.

The jumplike increase in the number of particles in the region of injection of the quenching jet is caused by flow compression by the side jets, by the increase in the particle number density, and, hence, by the increase in the coagulation rate. Stabilization of the particle size is caused by the decrease in the number of particles and simultaneous increase in the flow (and particle) velocity in the region behind the quenching jet (see Fig. 2a). After the quenching jet is interrupted, the particle velocity decreases from 40 m/s (see Fig. 2a) to 25 m/s (see Fig. 2b), which leads to a further increase in the particle size due to coagulation (see Fig. 2b). The calculations were performed with the use of the model of titanium tetrachloride conversion [2] verified on the basis of the experimental data [3].

The process of silicon tetrachloride conversion was calculated for the following parameters of reactor operation: $T_1 = 4300$ K, $Q_1 = 1.23$ g/s, $T_2 = 300$ K, $Q_2 = 0.47$ g/s, $T_3 = 300$ K, and three values of the quenching jet flow rate $Q_3 = 1.8$, 4.1, and 8.1 g/s. This study of the possibility of controlling the physical and chemical properties of the SiO_2 powder and the morphology of its particles simultaneously serves for validation of the model used. Figure 3 shows the distributions of the particle diameter averaged over the cross section. Upstream from the slot of quenching jet injection, an increase in the flow rate of the quenching jet and, hence, a decrease in the main flow temperature lead to reduction of the rates of all reactions, resulting in reduction of the size of particles being synthesized.

The table summarizes the results of the analysis of the microstructure and physical and chemical properties of powder samples consisting of amorphous SiO_2 particles (S_{BET} is the specific surface area, d_{BET} is the mean particle diameter calculated on the basis of the specific surface area, and C_{Cl} is the fraction of contaminating chlorine in the powder sample).

Figure 4a shows the agglomerates of the silicon oxide powder at the microscale, which were obtained for $Q_3 = 8.1$ g/s. It is seen that the agglomerate sizes are several micrometers. Figures 4b–4d show the agglomerates at the nanoscale for different flow rates of the quenching jet.

A comparison of the particle diameters obtained in the computations (see Fig. 3) and experiments (see the table) show that the normalized error is 7–8%, which proves that the models of silicon tetrachloride conversion and silicon dioxide synthesis are fairly adequate.

The analysis of the samples shows that it is possible to control the physical and chemical properties of the powder and the morphology of its particles. The specific particle surface area increases, whereas the characteristic particle size decreases with reduction of the ratio of the hydrodynamic pressures of the quenching jet and hot main flow. The fraction of contaminating chlorine in the final product also decreases owing to dilution of the flow by the quenching jets.

The synthesis of composite particles was calculated under the following conditions. The geometric characteristics of the reactor were $L_R = 600$ mm, $d_R = 32$ mm, $L_C = 38$ mm, $d_C = 14$ mm, $L_T = 33$ mm, and $\alpha = 15^\circ$; the coordinates of the middle lines of the slots for side jet injection were $z_1 = 28$ mm and $z_2 = 192$ mm; the setup operation regime parameters were $T_1 = 4500$ K, $Q_1 = 1$ g/s, $T_2 = 300$ K, $Q_2 = 4.0$ g/s, $T_3 = 300$ K, and $Q_3 = 20$ g/s; the $TiCl_4$ flow rate in the side jet was 0.016 g/s, and the $SiCl_4$ flow rate in the side jet was 0.004 g/s.

Figure 5 shows the distribution of the mean weighted particle diameter based on the number of particles along the reactor channel

$$d_i = \frac{1}{N_i} \sum_j d_{ij} N_{ij} \qquad \Big(N_i = \sum_j N_{ij} \Big),$$

and also the distribution of the particle number density obtained with the use of the model of a completely coated core.

In contrast to individual injection of $TiCl_4$ and $SiCl_4$ vapors (see [5]), in the case of joint injection of the reagents through the first side slot, there is practically no region where the titanium dioxide particles increase in size, resulting in synthesis of particles with the core whose size is small as compared to the shell thickness. The degree of mixing of the titanium dioxide and silicon dioxide particles in the gas phase is higher than that in the region of mixing of the second side jet and the main flow in the case of individual injection. As a result, the number of composite particles at the exit from the working region is significantly greater. If there is the second jet

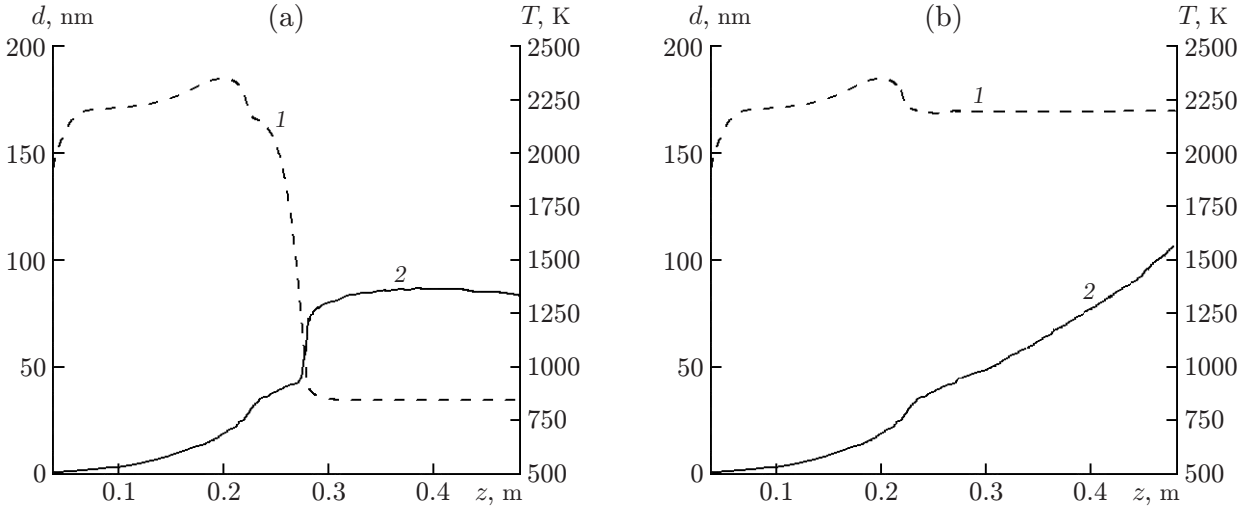

Fig. 2. Distributions of the temperature averaged over the cross section (*1*) and mean weighted particle diameter (*2*) along the reactor channel in the presence of the quenching jet ($Q_3 = 3{,}6$ g/s) (a) and at the time $\Delta t = 0.05$ s after jet interruption (b).

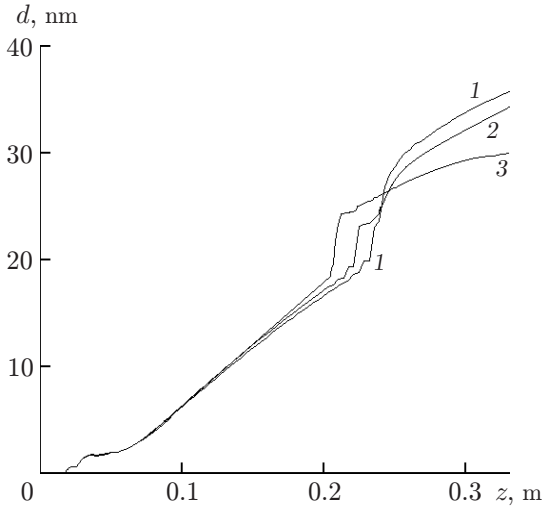

Fig. 3. Distributions of the particle diameter averaged over the cross section along the reactor channel for different values of the flow rate of the quenching jet: $Q_3 = 1.8$ (*1*), 4.1 (*2*), and 8.1 g/s (*3*).

Table 1. Microstructure and physical and chemical properties of the SiO_2 powder samples

Q_3, g/s	S_{BET}, m^2/g (Sorbi-M device)	d_{BET}, nm	C_{Cl} (at.), % (electron diffractometry, JEM-2200FS)
1.8	70	39.0	0.38
4.1	73	37.4	0.12
8.1	96	28.4	0.13

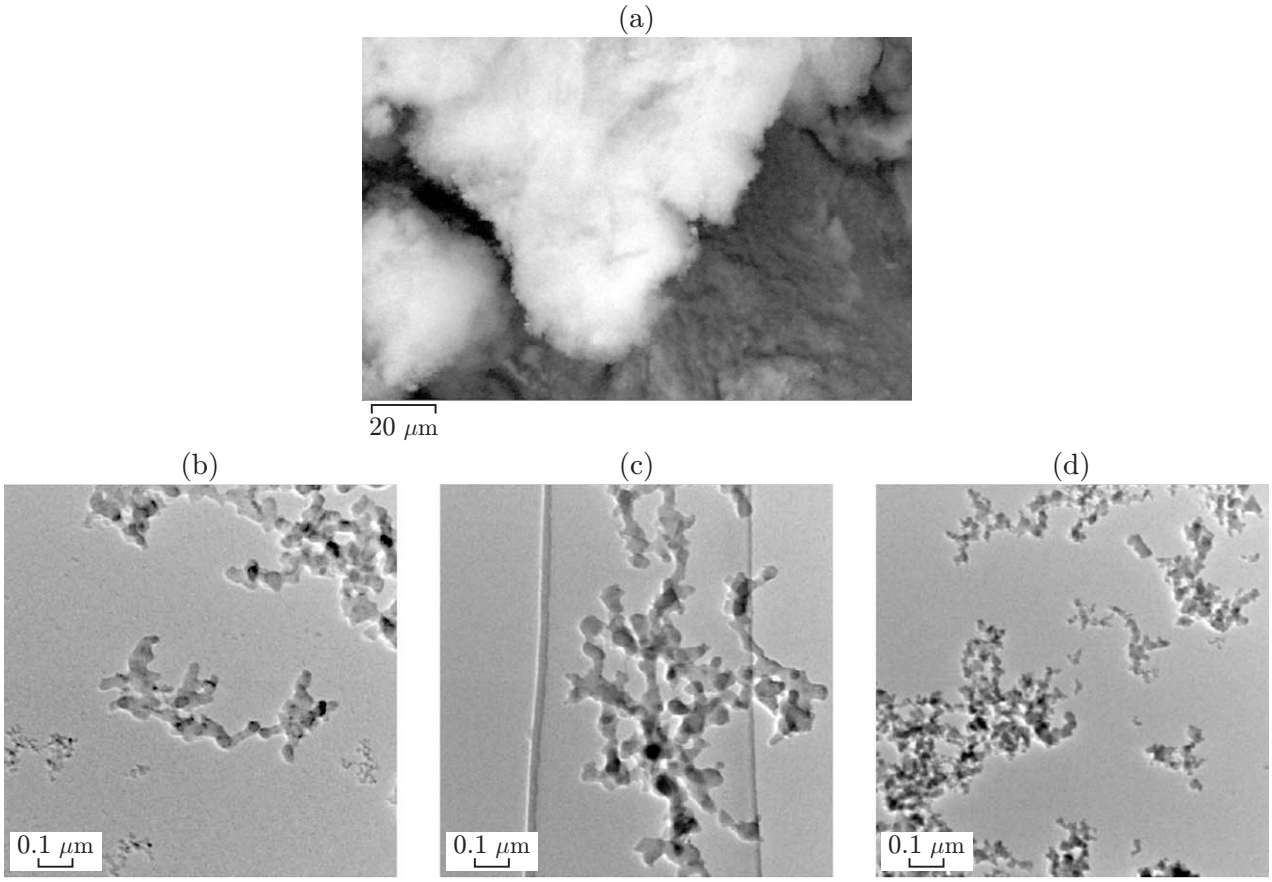

Fig. 4. Agglomerates of the SiO_2 powder at the microscale (taken by the Carl Zeiss EV050 XVP raster electron microscope) (a) and nanoscale (high-resolution JEM-2200FS transmission electron microscope) (b–d) for different flow rates of the quenching jet: (a, d) $Q_3 = 8.1$ g/s; (b) $Q_3 = 1.8$ g/s; (c) $Q_3 = 4.1$ g/s.

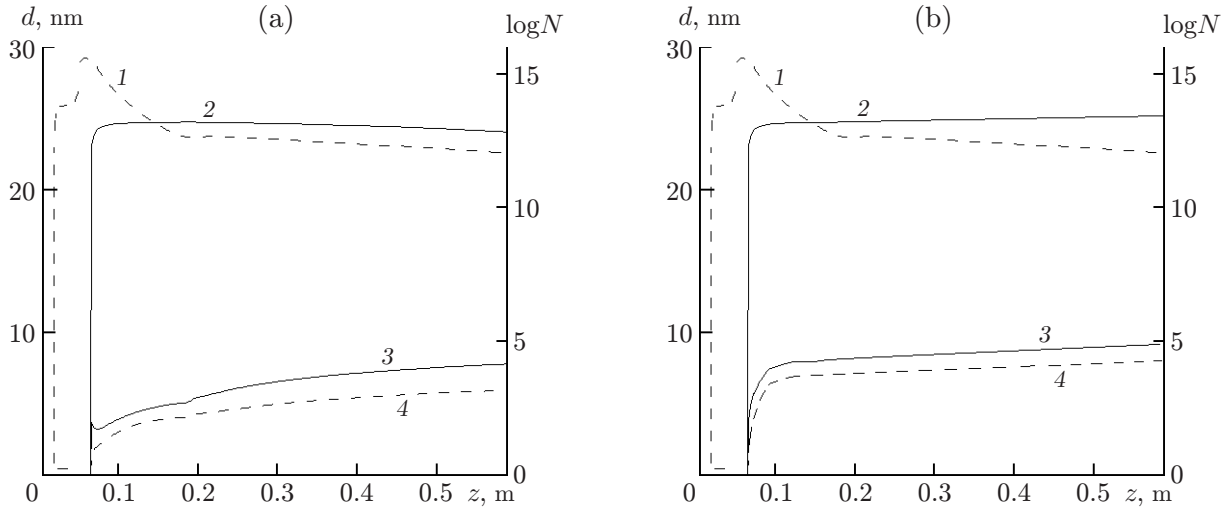

Fig. 5. Distributions of the mean weighted particle diameter along the reactor channel and particle number density obtained with the use of the model with a completely coated core: (a) in the absence of the side jet; (b) in the presence of the side jet; logarithm of the number density of TiO_2 particles (*1*), logarithm of the number density of composite particles (*2*), diameter of composite particles (*3*), and diameter of the core of composite particles (*4*).

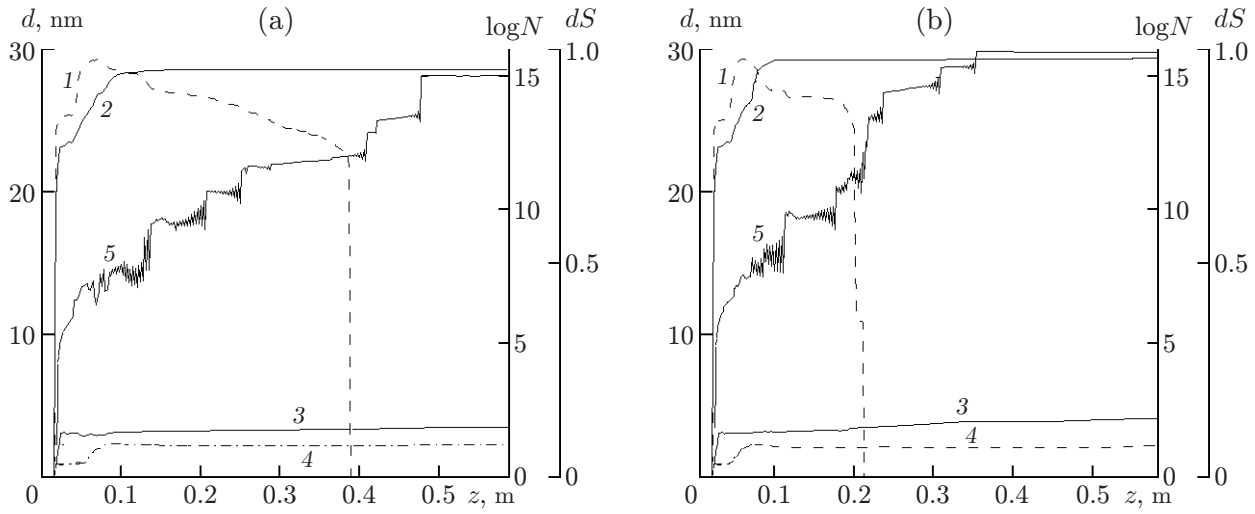

Fig. 6. Distributions of the mean weighted particle diameter, particle number density, and mean weighted fraction of the particle surface coated by SiO_2 along the reactor channel obtained with the use of the model with a partially coated core: (a) in the absence of the side jet; (b) in the presence of the side jet; logarithm of the number density of TiO_2 particles (*1*), logarithm of the number density of composite particles (*2*), diameter of composite particles (*3*), diameter of the core of composite particles (*4*), and fraction of the particle surface area coated by SiO_2 (*4*).

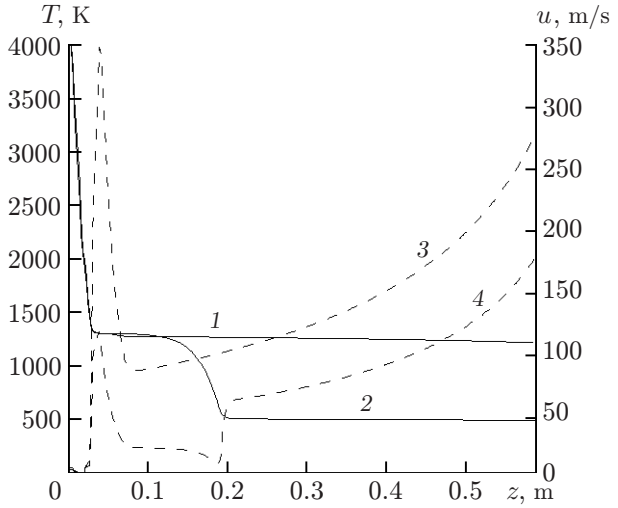

Fig. 7. Distributions of the temperature (*1, 3*) and streamwise velocity component (*2, 4*) averaged over the cross section along the reactor channel: in the absence of the second side jet (*1, 2*) and in the presence of the second side jet (*3, 4*).

(see Fig. 2), the flow ahead of the injection region is decelerated, which increases the time of particle residence in this region; correspondingly. the core size of the composite particles increases because the TiO_2 particles coagulate. In this case, the shell thickness is smaller than that in the case without the second side jet.

Figure 6 shows the results calculated for the same scheme of injection of the reagents and side jets, but with the model of synthesis with a partially coated core. It is seen in Figs. 5 and 6 that the number of composite particles at the reactor exit computed with the use of the model with completely coated particles is smaller by several orders of magnitude than the number of composite particles obtained by using the model with partially coated particles. The results predicted by these two models also display qualitative differences. It is seen in Fig. 6 that there are no titanium dioxide particles at the reactor exit. Owing to coagulation of TiO_2 particles and the process of shell formation transforming these particles to composite particles, there are no pure titanium dioxide particles left in

the flow, which is evidenced by the character of curve *1* in Fig. 6. In the case with the model of a partially coated core, the process of transformation of TiO_2 particles to composite particles in the stagnation region upstream of the second side jet prevails over the coagulation process even if the fraction of the surface area coated by SiO_2 is small. Therefore, the core size is smaller than that in the absence of the side jet (cf. Figs. 6a and 6b), while the shell thickness is greater. This situation is opposite to that predicted by the model with a completely coated core (cf. Figs. 5a and 5b). The shape of curve *5* in Fig. 6, which describes the behavior of the mean weighted fraction of the particle surface area coated by SiO_2 (presence of steps, non-monotonicity) is explained by the inherent constraint of the model on the minimum shell thickness equal to the diameter of silicon dioxide monomers and possible reduction of the coated area due to the transformation of TiO_2 particles to composite particles, which have a small area of the coated core surface.

Figure 7 shows the distributions of the flow temperature and velocity along the reactor channel in the cases with and without the side jet during synthesis of composite particles. It is seen that the side jet decelerates the flow at the reactor channel exit and reduces the gas temperature. These events affect the time of particle residence in the active zone, reaction rates, and, as a consequence, the core size and shell thickness.

CONCLUSIONS

The paper describes the results of studying the influence of the quenching air jet on the physical and chemical properties and morphology of titanium dioxide particles, silicon dioxide particles, and composite TiO_2–SiO_2 particles synthesized by a one-stage chloride method in a flow-type plasma-chemical reactor. This influence is induced by the changes in the flow characteristics (temperature, velocity) in the reactor channel and by the emergence of additional circulation regions in the vicinity of jet injection. The possibility of controlling the size of the synthesized particles by means of changing the quenching jet parameters is demonstrated. The results of mathematical modeling of particle synthesis for the cases of TiO_2 and SiO_2 particles are found to agree well with experimental results.

This work was partly performed within the framework of the Program of Fundamental Research of the State Academies of Sciences in 2013–2020 (Project No. AAAA-A17-117030610120-2) and was partly supported by the Russian Foundation for Basic Research (Grant No. 18-08-00219a).

REFERENCES

1. S. M. Aulchenko, A. F. Latypov, and N. N. Yanenko, "Application of the Projection Method for Constructing the Contour of a Body with the Minimum Drag," Izv. Ross. Akad. Nauk, Mekh. Zhidk. Gaza, No. 2 108–113 (1985).
2. S. M. Aulchenko, "Control of the Growth of Titanium Dioxide Nanoparticles in a Plasma-Chemical Flow Reactor," Inzh.-Fiz. Zh. **86** (5), 967–973 (2013).
3. E. V. Kartaev, V. P. Lukashov, S. P. Vashenko, et al., "An Experimental Study of the Synthesis of Ultrafine Titania Powder in Plasmachemical Flow-Type Reactor," Intern. J. Chem. Reactor Engng. **12** (1), 1–20 (2014). DOI: 10.1515/ijcre-2014-0001.
4. E. V. Kartaev, S. M. Aulchenko, and V. A. Emelkin, "Experimental and Numerical Study of High-Temperature Synthesis of Nanosized Silica Particles in Flow-Type Plasmachemical Reactor," in *Abstr. of the 14th Intern. Conf. "Gas discharge plasmas and their applications,"* Tomsk (Russia), September 15–21, 2019 (TPU Publ. House, Tomsk, 2019, P. 182).
5. S. M. Aulchenko and E. V. Kartaev, "Modeling the One-Stage Synthesis of Composite Particles of the Nucleus–Shell Type in Separate Oxidation of Titanium and Silicon Tetrachlorides in a Plasmachemical Reactor," Inzh.-Fiz. Zh. **93** (1), 114–120 (2020) [J. Eng. Phys. Thermophys. **93**, 108–113 (2020].
6. S. M. Aulchenko and E. V. Kartaev, "Modeling of Synthesis of Composite "Core–Shell" Particles on the Basis of Joint Oxidation of Titanium and Silicon Tetrachlorides in a Plasma-Chemical Reactor," Prikl. Mekh. Tekh. Fiz. **61** (4), 77–83 (2020) [J. APpl. Mech. Tech. Phys. **61** (4), 566–572 (2020)].
7. A. M. El-Toni, S. Yin, and T. Sato, "Control of Silica Shell Thickness and Microporosity of Titania — Silica Core — Shell Type Nanoparticles to Depress the Photocatalytic Activity of Titania," J. Colloid Interface Sci. **300** (1), 123–130 (2006).

8. I. A. Siddiquey, T. Furusawa, M. Sato, et al., "Control of the Photocatalytic Activity of TiO_2 Nanoparticles by Silica Coating with Polydiethoxysiloxane," Dyes Pigments. **76** (3), 754–759 (2008).
9. A. Teleki, B. Buesser, M. C. Heine, et al., "Role of Gas-Aerosol Mixing During in Situ Coating of Flame-Made Titania Particles," Industr. Engng Chem. Res. **48** (1), 85–92 (2009).
10. B. Buesser and S. E. Pratsinis, "Design of Gas-Phase Synthesis of Core-Shell Particles by Computational Fluid — Aerosol Dynamics," AIChE J. **57** (11), 3132–3142 (2011).
11. E. A. Grinyaeva, B. Sh. Kochkorov, D. V. Ponomarev, et al., "Plasma-Chemical Synthesis of Crystalline Nano-Sized Composite Oxides," Izv. Tom. Politekh. Univ., Ser. Khimiya, **317** (3), 33–37 (2010).
12. P. V. Grishin, V. E. Katnov, G. S. Stepin, et al., "Gas-Phase Synthesis of Composite Particles with the Core–Shell Structure on the Basis of Silicon (IV) and Zinc," Vestnik Kazan. Tekhnol. Univ., **19** (14), 56–60 (2016).
13. S. H. Ehrman, S. K. Friedlander, and M. R. Zachariah, "Characteristics of SiO_2/TiO_2 Nanocomposite Particles Formed in a Premixed Flat Flame," J. Aerosol Sci. **29** (5/6), 687–706 (1998).
14. A. Kolesnikov and J. Kekana, "Nanopowders Production in the Plasmachemical Reactor: Modelling and Simulation," Intern. J. Chem. Reactor Engng. **9**, Article A83 (2011).
15. H. K. Park and K. Y. Park, "Control of Particle Morphology and Size in Vapor-Phase Synthesis of Titania, Silica and Alumina Nanoparticles," KONA Powder Particle J., No. 32, 85–101 (2015).
16. T. G. Elizarova, *Quasi-Gas-Dynamic Equations and Methods of Viscous Flow Calculation* (Nauch. Mir, Moscow, 2007) [in Russian].